NANO: Brief Reports and Reviews
Vol. 2, No. 3 (2007) 149–156

World Scientific
www.worldscientific.com

RIPENING OF SILVER NANOPARTICLES ON CARBON NANOTUBES

LIYING ZHU*, GANHUA LU†, SHUN MAO‡ and JUNHONG CHEN§
Department of Mechanical Engineering, University of Wisconsin-Milwaukee
3200 N. Cramer St., Milwaukee, WI 53211, USA
**lyzhu@uwm.edu*
†*ganhualu@uwm.edu*
‡*shunmao@uwm.edu*
§*jhchen@uwm.edu*

DMITRIY A. DIKIN
Department of Mechanical Engineering, Northwestern University
2145 Sheridan Road, Evanston, IL 60208, USA
d-dikin@northwestern.edu

XINQI CHEN
NUANCE Center, Northwestern University, Evanston, IL 60208, USA
xchen@northwestern.edu

RODNEY S. RUOFF
Department of Mechanical Engineering, Northwestern University
2145 Sheridan Road, Evanston, IL 60208, USA
r-ruoff@northwestern.edu

Received 9 March 2007
Revised 2 May 2007

An electrostatic-force-directed-assembly technique was used to coat multiwalled carbon nanotubes (MWCNTs) with aerosol Ag nanoparticles produced from a mini-arc plasma source. The deposition of Ag nanoparticles onto CNTs was confirmed by transmission electron microscopy (TEM), high-resolution TEM, scanning electron microscopy, and X-ray photoelectron spectroscopy. Ripening of Ag nanoparticles on CNTs was observed via successive TEM imaging after heating the nanoparticle–nanotube hybrid structures in air to three different temperatures ranging from 100°C to 300°C. With temperatures at and above 200°C, the areal density of Ag nanoparticles decreased and the average particle size increased. In particular, migration and coalescence of Ag nanoparticles have been observed at this relatively low temperature, which suggests a van der Waals nanoparticle–nanotube interaction.

Keywords: Ripening; Ostwald ripening; migration and coalescence; electrostatic-force-directed-assembly; van der Waals force; Ag nanoparticles; carbon nanotubes; hybrid nanostructures.

§Corresponding author.

1. Introduction

Because of their physical, electronic, and mechanical properties, metal and carbon nanotube (CNT) hybrid structures are promising materials for next-generation electronic devices with low-resistance ohmic contacts.[1] CNTs coated with metal nanoparticles (NPs) are of potential interest for catalysis including in fuel cells,[2] for hydrogen storage,[3] and as photoelectrochemical cells.[4] In addition, metal NPs/CNT hybrid structures show potential for use in sensing devices.[5] In general, the binding between the nanoparticle and the CNT surface can be either covalent[6] or noncovalent.[7] Covalent bonding between the nanoparticle and the CNT has to date been obtained through different acid treatments to create such linking groups as carboxyl (−COOH), carbonyl (−C=O) and hydroxyl (−OH). However, mechanical and particularly electronic transport properties of the nanotubes may significantly degrade after acid treatment due to the introduction of defects.[6] Noncovalent attachment of nanoparticles is more likely to preserve the unique properties of low-defect CNTs.[7]

Recently, we developed a generic method to assemble nanoparticles of various materials onto CNTs based on electrostatic-force-directed-assembly (ESFDA).[8] This method relies on an enhanced electric field near the CNT surface through an applied dc bias on the CNT to attract oppositely charged nanoparticles. Since the assembly is performed at room temperature in inert gas, the chance of having noncovalent binding between nanoparticle and nanotube is enhanced, relative to the use of higher temperatures or more reactive environments. The behavior of the CNT/NP structure at higher-than-ambient temperatures in air is also relevant for many applications. For example, metal oxide gas sensors are typically operated at elevated temperatures (200–500°C) to maximize the sensitivity.[9] Thus, following creation of the hybrid structures by the aerosol deposition at room temperature and under inert gas, it is useful to understand how particle distribution, binding, and morphology are influenced by heating in air.

Ag nanoparticles were coated onto multiwalled CNTs (MWCNTs) and characterized using transmission electron microscopy (TEM), high resolution TEM (HRTEM), scanning electron microscopy (SEM), and X-ray photoelectron spectroscopy (XPS). The evolution of the hybrid structure was studied using TEM imaging after particular heating cycles were applied in air. At and above 200°C, significant ripening of Ag nanoparticles on CNTs was observed for the first time. The smaller Ag nanoparticles were consumed by the larger nanoparticles, which resulted in a decrease of the areal density of Ag nanoparticles accompanied by a simultaneous increase of the average nanoparticle size. Further analyses of the successive TEM images indicated that some Ag nanoparticles actually migrated and coalesced with neighboring particles on the CNT surface. Such a migration and coalescence at this low temperature suggests a weak interaction between CNTs and Ag nanoparticles.

2. Experimental Procedure

The aerosol Ag nanoparticles were generated through physical vaporization of a solid Ag precursor wire (99.999% purity, ESPICorp Inc.) using a mini-arc plasma generated between a tungsten cathode and a graphite anode.[10] The as-produced nanoparticles were nonagglomerated and crystalline with a relatively broad size distribution ranging from a few to tens of nanometers. A fraction of the nanoparticles were electrically charged through the thermal plasma or the thermionic emission of electrons from the nanoparticle surface,[11] which significantly facilitates the subsequent electrostatic assembly of nanoparticles onto CNTs.

The electrostatic-force-directed assembly (ESFDA)[8] was accomplished between a grounded metal tube that introduced the aerosol particles and a dc-biased nickel TEM grid (400 mesh, Ted-Pella, Inc.). The TEM grid was covered with MWCNTs purchased from Alfa Aesar (Stock # 43839). Nickel was chosen due to its resistance to oxidation in air and its thermal stability in the temperature range used in this study (up to 300°C). A precision-machined ceramic spacer maintained a 2-mm gap between electrodes. The ESFDA was accomplished at room temperature and one atmosphere pressure of a carrier gas (Ar/N_2; flow rate of 5.15 liters per minute) and with an applied dc voltage of $-2\,kV$ on the CNTs. The electric field near the CNTs was significantly enhanced due to their small diameters and charged Ag nanoparticles were attracted to the outer surface of the CNTs.[8,12]

The product structures were analyzed using TEM, HRTEM, SEM, and XPS, all of which confirmed the successful assembly of Ag NP/CNT hybrid structures. The structures were then further

studied after exposure to different heating treatments in air. A Hitachi H 9000 NAR transmission electron microscope was used for TEM and HRTEM analyses. This TEM has a point resolution of 0.18 nm at 300 kV in the phase contrast HRTEM imaging mode. The SEM used was a Nova 600 NanoSEM (FEI Co.) equipped with a transmission electron detector. XPS was performed on a HP5950 ESCA spectrometer with monochromatic AlKα radiation as the X-ray source.

To understand the influence of exposure of the hybrid structures to elevated temperatures in air, regions on the TEM grid were identified and imaged prior to heating. The location of each region was determined by its position with respect to the central mark of the grid for a given grid orientation. After the target regions were selected, the TEM grid containing the Ag NP/CNT hybrid structures were placed into an oven with a preset temperature and held for one hour (h) at that temperature. At the end of each heating cycle, the sample was removed from the oven, quickly cooled to room temperature, and immediately imaged with the TEM. Due to the small mass of the grid, both the heating and cooling rates are expected to be quite high. The first of the three heating cycles was performed with a preset oven temperature of 100°C, the second at 200°C, and the third at 300°C. The same sample was used for each cycle. The results of these experiments are discussed below.

3. Results and Discussion

Low-magnification TEM and HRTEM images showed Ag nanoparticles decorating the MWCNTs, thus confirming their assembly by ESFDA. Figure 1(a) is a TEM image of clean MWCNTs that are seen to have a diameter of about 20–40 nm and a length of several micrometers. The MWCNT surface is very smooth, as also seen in the corresponding HRTEM image in Fig. 1(b). Figure 1(c) is a TEM image of MWCNTs coated with Ag nanoparticles, which are distributed more or less uniformly on the external surface of the CNTs. This hybrid structure is shown at higher magnification in the HRTEM image, Fig. 1(d). The measured lattice fringe spacings of 0.20 and 0.23 nm in these Ag nanoparticles correspond to the (200) and (111) crystal planes, respectively. The average diameter of the Ag nanoparticles is less than 10 nm, much smaller than their average size in the aerosol prior to deposition onto the MWCNTs. This is due to the nanoparticle size selection that occurs during the assembly.[8] Figure 1(f) is an SEM image of clean MWCNTs and Fig. 1(g) shows the same CNTs uniformly covered with Ag nanoparticles.

The Ag NP/CNT hybrid structures were further analyzed using XPS. Figure 2(a) is a survey spectrum of the hybrid nanostructure, which shows strong signals of Ag and C. No evidence for oxidation of the Ag nanoparticles is observed, which is consistent with our prior X-ray diffraction study on as-produced Ag nanoparticles.[10] The C signal with a binding energy of 284.5 eV is from the CNTs and corresponds to the C 1s core level spectrum. Figure 2(b) shows the Ag $3d_{5/2}$ and $3d_{3/2}$ doublets with the binding energies of 368 eV and 373.9 eV, respectively, which are typical values for bulk Ag.[13]

We now turn to a discussion of the heat treatments in air. At a temperature as low as 200°C, smaller Ag particles move and merge with larger Ag particles. Ripening evidently has occurred during the one hour of heating. As a result, the areal density of Ag nanoparticles on the CNT decreases while the average diameter ($\bar{D}_p$) of Ag nanoparticles increases. Figure 3 is a TEM image of the original sample of CNTs covered with Ag nanoparticles of an average diameter of 9.0 nm. The Ag nanoparticle size distribution shown in the inset was estimated by TEM. Figure 4 shows a sequence of TEM images of the same Ag NP/CNT sample heated to different temperatures (left column), the corresponding Ag particle size distributions estimated by TEM (inset), and the HRTEM images of selected areas (right column).

Figures 4(a), 4(c), and 4(e) are TEM images of the sample after being heated to 100°C for 1 h, then to 200°C for 1 h, and finally to 300°C for 1 h, respectively. The corresponding average Ag nanoparticle diameter increases from 9.0 nm at room temperature to 9.4 nm, 11.7 nm, and 19.7 nm at 100°C, 200°C, and 300°C, respectively. Figures 4(b), 4(d), and 4(f) are the HRTEM images of the Ag particles circled in the corresponding low-magnification TEM images. At 100°C, there seems to be an amorphous layer covering the Ag nanoparticle surface, which is likely from the low-temperature oxidation of Ag. At a temperature above 200°C, silver oxides are known to decompose to form metallic silver.[14] As a result, the amorphous layer disappeared and only pure Ag nanocrystals were observed after the same sample was heated to 200 and 300°C. The lattice fringes shown in Figs. 4(b), 4(d), and 4(f)

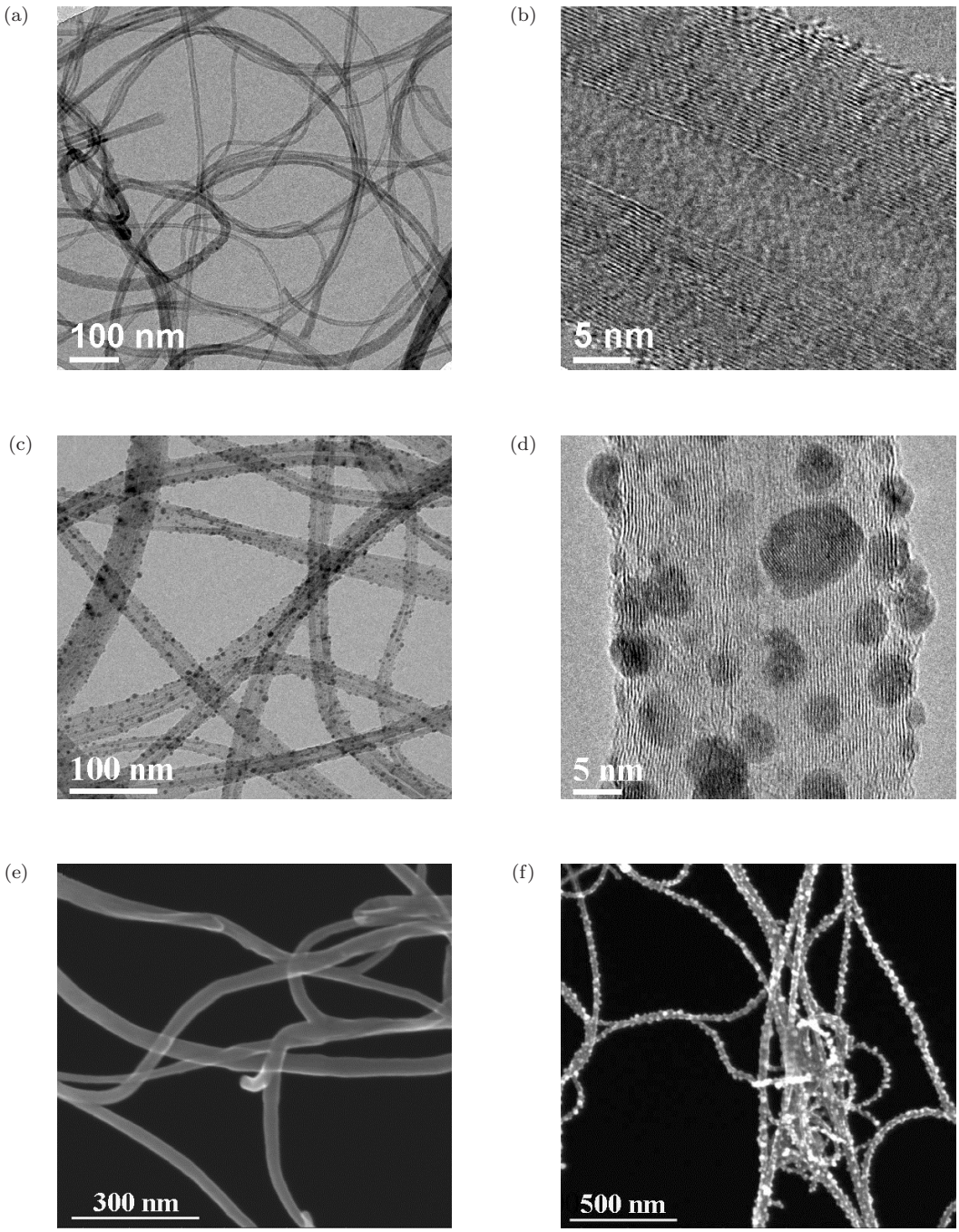

Fig. 1. Low-magnification TEM and HRTEM images of MWCNTs before assembly ((a) and (b)) and MWCNTs coated with Ag nanoparticles ((c) and (d)); SEM images of MWCNTs (e) before assembly and (f) after assembly of Ag nanoparticles.

are all corresponding to those of Ag. Figure 4(e) also shows that some portions of the CNTs become thinner; this is likely due to the e-beam irradiation during TEM imaging.[15]

Images obtained at room temperature (Fig. 3) and after 1 h of heating at 100°C (Fig. 4(a)) show that there is no obvious change in the Ag nanoparticle distribution. A clear change in the Ag nanoparticle distribution is observed after the sample is next heated to 200°C for 1 h (Fig. 4(c)). During the 1 h heating, the following changes are observed for the labeled particles: Particle 1 grows bigger to particle 1′; particles 3 and 4 migrate and merge with particle 2 to form larger particle 2′; particles 5 and 6 merge to form particle 6′; and particle 7 grows into particle 7′. The full coalescence

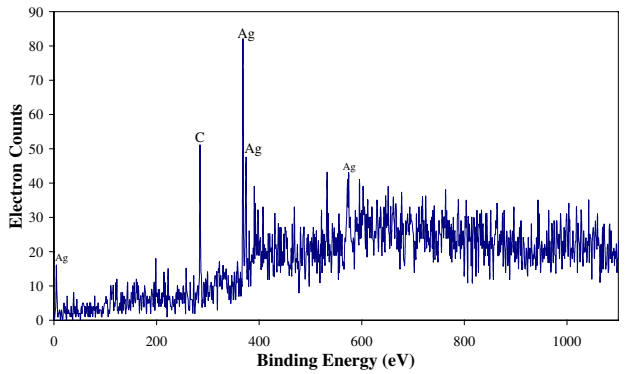

(a)

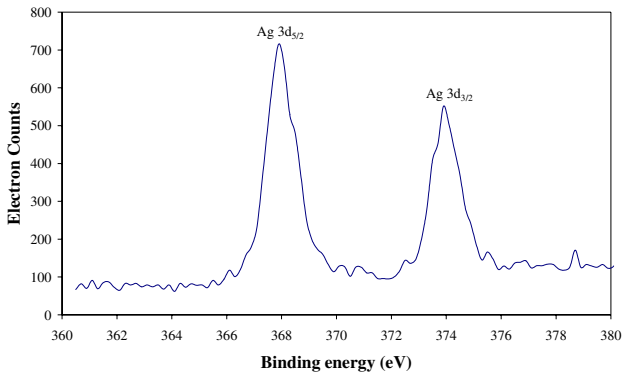

(b)

Fig. 2. XPS spectrum of (a) C 1s core level and (b) Ag 3d core level spectrum of MWCNTs coated with Ag nanoparticles.

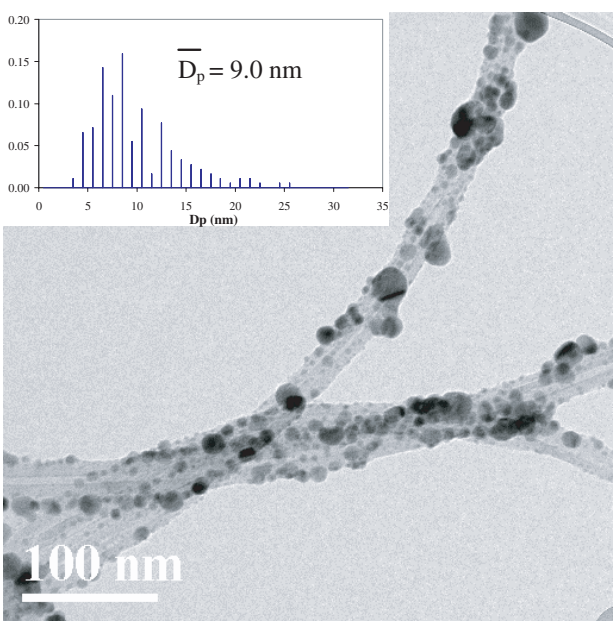

Fig. 3. TEM image of the original Ag NP/CNT structure at room temperature with the corresponding Ag nanoparticle size distribution (particle number fraction versus particle diameter) shown in the inset.

of particle 2′ is not achieved as can be inferred from its elongated morphology. The change is most obvious after the sample is finally heated to 300°C for 1 h (Fig. 4(e)); the increase in the average Ag particle size and the decrease in the nanoparticle areal density are quite significant. Larger Ag nanoparticles grow even larger by absorbing smaller Ag nanoparticles from the CNT surface. For example, particles 1′, 2′, 6′, and 7′, merge together and fully coalesce to form a larger particle 2″ with a nearly spherical shape. In addition, particle 2″ had migrated down and to the left on the CNT surface during the heating cycle.

Smaller nanoparticles on the CNT surface may be energetically less stable than larger ones due to their relatively larger surface to volume ratio. As a result, the transformation of smaller particles into larger ones could be energetically favorable on the CNT surface. In addition, smaller nanoparticles are likely to diffuse more readily than larger ones and so the growth of the larger particles could simply be a consequence of the smaller ones moving and colliding with the larger particles to form even larger particles. Coalescence of the merged larger particles can also be inferred based on the TEM images, as the observed particles are nearly spherical as shown in Fig. 4(e). Although the vapor pressure of Ag nanoparticles is known to be higher than that of bulk Ag,[16] at these relatively low temperatures and for the total exposure time of 3 h, it is unlikely that a significant fraction of Ag is lost (if any) by atomic evaporation.

The ripening of Ag nanoparticles on CNTs can be anticipated from the studies of Ag clusters/particles located on other surfaces[17–19] or embedded in polymer films.[20] Two possible mechanisms are known to be responsible for the ripening process, namely Ostwald ripening and particle migration and coalescence.[21,22] In an Ostwald ripening process, atomic species from smaller particles transport to larger particles either by surface diffusion along the substrate or by vapor phase diffusion due to the difference in the chemical potentials between smaller and larger particles. Under the particle migration and coalescence mechanism, smaller particles migrate on the substrate surface and then collide/coalesce with larger particles.

Although it is difficult to obtain a detailed mechanistic insight based solely on the change in particle size distribution before and after heating,[23] additional comparison of successive TEM images

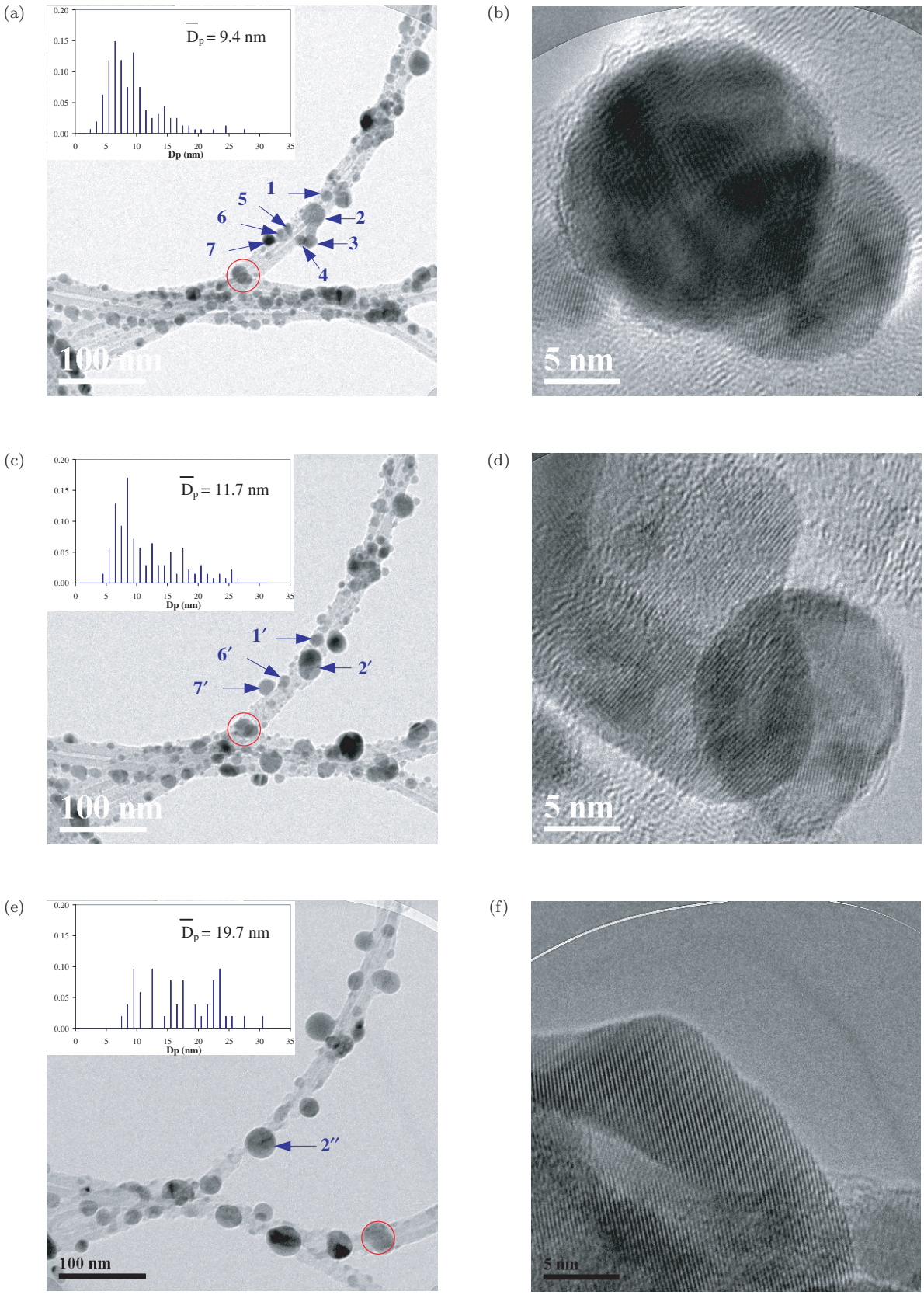

Fig. 4. Left column: Low-magnification TEM images and the corresponding Ag nanoparticle size distributions (inset) of the Ag NP/CNT structure heated in air to (a) 100°C, then (c) 200°C, and then finally to (e) 300°C. Right column: HRTEM images of the area marked in the circle in the corresponding low-magnification TEM images.

has allowed us to infer the occurrence of Ag particle migration and coalescence in our experiments. Of course, we cannot exclude the possibility of Ostwald ripening, and observation using an *in situ* heating experiment inside a TEM chamber might further elucidate the mechanism.[24] There is the possibility of competition between possible thermodesorption of the whole Ag nanoparticle from the CNT surface versus migration of the nanoparticle on the CNT surface; the rates for both are expected to increase with increasing temperature. The TEM images obtained after the three 1 h thermal treatments at 100, 200, and 300°C show that surface migration of Ag particles occurs more readily than thermodesorption of Ag nanoparticles, even at 300°C. The more ready surface migration thus leads to the ripening of the Ag nanoparticles.

The migration of Ag nanoparticles at these relatively low temperatures suggests a weak interaction between Ag nanoparticles and CNTs. It is well known that some transition elements chemically bond to carbon.[25] This is attributed to the distribution of *d* electrons in such transition elements. Since Ag atoms have no *d* vacancy orbitals, they have very weak affinity for bonding with carbon atoms.[26] As a result, Ag nanoparticles are most likely attached to CNTs through van der Waals forces instead of chemical bonds.[27]

The reader might note that to date it has not been possible to measure, for example, the binding energy of individual C_{60} molecules on a graphite surface,[28] because C_{60} does not thermally desorb from the surface at low coverage. It is of interest that C_{60} diffuses on a highly ordered pyrolytic graphite (HOPG) surface as 2D gas, which "defeated" efforts to obtain the thermodynamic and kinetic parameters for desorption of isolated C_{60} molecules from the graphite surface; rather, the desorption was found to be from islands that had grown on the surface from lateral diffusion and binding of C_{60} molecules.[a] Our experiments suggest that the Ag nanoparticles are trapped on the CNT surface through van der Waals forces and are unlikely to leave the surface at the temperatures employed. Because the CNT surface is relatively smooth, we speculate that the barrier for thermally activated migration of Ag nanoparticles is low and thus favors surface migration and ripening.

4. Conclusion

Aerosol Ag nanoparticles were assembled onto the surface of MWCNTs at room temperature in inert gas using a new electrostatic-force-directed-assembly technique. The interaction between the Ag nanoparticle and the CNT was studied for 1 h exposures in air at temperatures of 100°C, 200°C, and 300°C. After each exposure, the same regions of the sample were imaged using a TEM. The observation by TEM imaging of ripening of Ag nanoparticles on CNTs at temperatures as low as 200°C for such exposure times suggests that the Ag nanoparticle is bound through van der Waals forces rather than with covalent bonds. This study hence sheds light on the properties of the nanoparticle–nanotube hybrid structure that are relevant to its potential applications, including at high temperatures. Although only Ag nanoparticles were considered in this study, the same heating method may be applied to evaluate the interactions between CNTs and nanoparticles of many other materials.

Acknowledgments

We thank Mildred S. Dresselhaus, Marija Gajdardziska-Josifovska, and Carol Hirschmugl for insightful discussions, Aleksandr Noy for helpful comments on the manuscript, Donald Robertson for technical support with TEM analyses, and Steven Hardcastle for assistance with XPS analyses. We also appreciate the insightful comments of the anonymous reviewers. TEM analyses were performed in the HRTEM Laboratory at University of Wisconsin-Milwaukee (UWM) and XPS analyses were done at the Advanced Analysis Facility of UWM. The financial support for this study was provided by the National Science Foundation (CTS-0604079 and DMI-0609059).

References

1. B. R. Azamian, K. S. Coleman, J. J. Davis, N. Hanson and M. L. H. Green, *Chem. Commun.* **4**, 366 (2002).
2. P. Santhosh, A. Gopalan and K. P. Lee, *J. Catal.* **238**, 177 (2006).

[a]Private communication with A. V. Hamza, work done in collaboration with M. Balooch, 2006, Lawrence Livermore National Laboratory.

3. P. Costa, K. S. Coleman and M. L. H. Green, *Nanotechnology* **16**, 512 (2005).
4. G. Q. Zhang, X. G. Zhang and Y. G. Wang, *Carbon* **42**, 3097 (2004).
5. Z. Y. Wu, L. G. Chen, G. L. Shen and R. Q. Yu, *Sens. Actuators B* **119**, 295 (2006).
6. A. Zamudio, A. L. Elias, J. A. Rodriguez-Manzo, F. Lopez-Urias, G. Rodriguez-Gattorno, F. Lupo, M. Ruhle, D. J. Smith, H. Terrones, D. Diaz and M. Terrones, *Small* **2**, 346 (2006).
7. T. Wang, X. G. Hu, X. H. Qu and S. J. Dong, *J. Phys. Chem. B* **110**, 6631 (2006).
8. J. H. Chen and G. H. Lu, *Nanotechnology* **17**, 2891 (2006).
9. Y. Shimizu and M. Egashira, *MRS Bull.* **24**, 18 (1999).
10. J. H. Chen, G. H. Lu, L. Y. Zhu and R. C. Flagan, *J. Nanopart. Res.* **9**, 203 (2007).
11. X. Wang, J. Hafiz, R. Mukherjee, T. Renault, J. Heberlein, S. L. Girshick and P. H. McMurry, *Plasma Chem. Plasma Process.* **25**, 439 (2005).
12. S. Podenok, M. Sveningsson, K. Hansen and E. E. B. Campbell, *Nano* **1**, 87 (2006).
13. C. D. Wanger, W. M. Riggs, L. E. Davis, J. F. Moulder and E. G. E. Muilenberg, *Handbook of X-Ray Photoelectron Spectroscopy* (Perkin-Elmer Corp., Eden Prairie, MN, 1978).
14. T. Shima and J. Tominaga, *Thin Solid Films* **425**, 31 (2003).
15. F. Banhart, J. X. Li and A. V. Krasheninnikov, *Phys. Rev. B* **71**, 241408(R) (2005).
16. M. Blackman, N. D. Lisgarten and L. M. Skinner, *Nature* **217**, 1245 (1968).
17. K. Morgenstern, G. Rosenfeld and G. Comsa, *Surf. Sci.* **441**, 289 (1999).
18. G. Rosenfeld, K. Morgenstern, I. Beckmann, W. Wulfhekel, E. Laegsgaard, F. Besenbacher and G. Comsa, *Surf. Sci.* **402**, 401 (1998).
19. R. Meyer, Q. Ge, J. Lockemeyer, R. Yeates, M. Lemanski, D. Reinalda and M. Neurock, *Surf. Sci.* **601**, 134 (2007).
20. A. Heilmann and J. Werner, *Thin Solid Films* **317**, 21 (1998).
21. P. Wynblatt and N. A. Gjostein, *Prog. Solid State Chem.* **9**, 21 (1975).
22. P. Wynblatt and N. A. Gjostein, *Acta Metallurgica* **24**, 1165 (1976).
23. A. K. Datye, Q. Xu, K. C. Kharas and J. M. McCarty, *Catal. Today* **111**, 59 (2006).
24. R. J. Liu, P. A. Crozier, C. M. Smith, D. A. Hucul, J. Blackson and G. Salaita, *Microsc. Microanal.* **10**, 77 (2004).
25. Y. Zhang, N. W. Franklin, R. J. Chen and H. J. Dai, *Chem. Phys. Lett.* **331**, 35 (2000).
26. E. Durgun, S. Dag, V. M. K. Bagci, O. Gulseren, T. Yildirim and S. Ciraci, *Phys. Rev. B* **67**, 201401 (2003).
27. Y. Zhang and H. J. Dai, *Appl. Phys. Lett.* **77**, 3015 (2000).
28. R. S. Ruoff and A. P. Hickman, *J. Phys. Chem. B* **97**, 2494 (1993).